#25-116
2025 AFS Proceedings ©American Foundry Society

Thermomechanical Properties of Shell Resin Coated Sands to Identify Cure Parameters

R. A. Makin, Z. Tay, & S. N. Ramrattan,
Western Michigan University, Kalamazoo, Michigan, USA

B. Gromala & K. Kerns
HA Group, Westmont, Illinois, USA

ABSTRACT

Shell molding technology remains an important part of metalcasting technology because it produces precision sand castings. As the ever-growing need to produce complex castings increases, so does the complexity of cores and molds. In order to accomplish near-net-shape casting with minimal defects, it is necessary to understand the thermal-mechanical effect undergone by the cured cores and molds at the superheat temperature for an alloy.

Aeration filling using free flowing resin coated shell sand offers a superior means to fill a core box. Aeration technology makes it possible to sand fill complex shapes, deep pockets, and thin sections in tooling that heretofore were not possible by conventional gravity or high-pressure blow. However, a conundrum remains in the determination of the optimal shell cure temperature. The foundry industry has generally used a visual criterion based on a cure color chart. This study points out the issues caused when using a subjective methodology.

This research study examines the effects of tight thermal curing parameters on both silica and ceramic shell sand systems. Laboratory testing equipment was utilized as opposed to the more laborious foundry casting trials. Productivity and quality issues such as shakeout and dimensional accuracy were used to determine optimal cure.

Aeration filled shell disc-shaped core specimens were fabricated and testing included scratch hardness, retained strength, and thermal distortion. With a shell aeration sand filling system, it is possible to produce cores and molds having superior abrasion resistance, strength, and thermal stability especially with ceramic sand.

Keywords: chemically bonded sand, cure color chart, Foundry 4.0, hot-box, precision sand, shell, thermal distortion, superheat, veining

INTRODUCTION

Precision sand molds and cores using chemical binders are the primary technology for the production of US automotive powertrains and certain aerospace components.[1] Problems with the sand casting process arise from variation. This can come from many sources such as grain size, grain shape, chemical composition, additives, and metallostatic pressure. Thus, sand has many potential sources of variation; but it is still subject to the pressures of delivering near-net shaped castings. Understanding those variations is a key issue for achieving good process control an important requirement in Foundry 4.0.[1]

As sand composites (mold and core media) come into contact with elevated temperatures, a thermal gradient will develop unique to that particular composite. When a sand composite comes in contact with elevated temperatures, the heat transferred causes thermomechanical movement and thermochemical reactions that result in dimensional changes at the mold-metal interface. At any given temperature these dimensional changes or thermal distortions are attributable to simultaneous changes in both the sand and the binder. Depending on the type of binder used and the temperature at any point in the sand plane, thermally induced reactions occur simultaneously along with sand expansion leading to significant distortions in the composite shape.[1-3]

A disc-shaped specimen (50 mm dia. x 8 mm thick) is an American Foundry Society (AFS) standard test specimen for chemically bonded sands.[4] An AFS standardized thermal distortion test (TDT) for measuring thermomechanical changes in chemically bonded sands employs the same simple geometry for a specimen.[1-4]

SHELL BACKGROUND

Developed in Germany during World War II, the Croning or shell process has undergone several stages of evolution.[5] Shell cores have always been associated with high-quality castings but concerns with emissions, odor and productivity opened the door in the 70's for many of today's nobake and coldbox binders. Advancements in

resin coated sand technology have addressed many of the concerns with emissions and productivity. Shell users have typically been concerned with free phenol, free formaldehyde and ammonia levels in their facility. By changing the chemical makeup of the reactants used to form and cure shell sand, suppliers now offer a resin coated shell sand with fewer hazardous air pollutants and reduced odor. Through research completed by Technikon in conjunction with the Casting Emission Reduction Program (CERP) and through comparative testing at the University of Northern Iowa, results have identified that developments in shell technology have made it cleaner and faster.[6]

The shell process gets its name from the ability to make either solid or hollow cores with a thin wall or shell, where the unused sand is removed from the core cavity or mold surface and reused. Making a core or mold follows five steps:

1. Gravity flow or blow resin coated shell sand is poured into a core box or onto a pattern for molding.
2. Heat from the tooling penetrates the sand to melt the resin that flows between the sand grains.
3. The tooling rotates upside down to allow the un-melted resin coated sand to fall out of the cavity to be collected and reused.
4. Heat curing to decompose a co-reactant.
5. Eject the cured shell.

The physical and chemical aspects of the cure need to be closely monitored. To make a core or mold, the reaction of the resin and co-reactant is initiated when resin coated shell sand contacts the heated tooling (temperature between 204-316C/400-600F).[5,6] The core or mold wall thickness is based on cure time. The heat causes the resin coating to melt and plastically flow between the sand grains. As the heat continues to transfer deeper into the core and intensifies, the co-reactant begins to break down into formaldehyde and ammonia. The formaldehyde is available to react with the phenol-formaldehyde based resin, which consumes the formaldehyde as it completely cross-links and transitions from a thermoplastic to a thermoset in the fully-cured, rigid state.[5,6]

When cure temperatures within the core box tool is improperly controlled this thermal imbalance is seen on the resin coated shell silica sand cores and molds (Fig. 1). The outcome of under to over curing in shell may result in a range of casting issues such as gas defects, veins, penetration, and rough as-cast surfaces.

In most cases the foundry industry uses a visual determination of shell cure subject to a cure temperature for a cure time. A complete cure is visually indicated by a degree of golden yellow to brown on a cure color chart (Fig. 2).

(a) Shell core package

(b) Cross section of cured shell core

Figure 1. Range of cured shell sand.

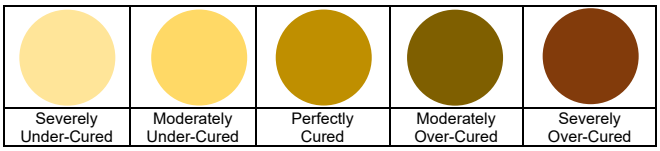

Figure 2. Shell cure color chart.

Today there are several alternative media such as ceramic sands that are available to the foundry industry for shell resin coating applications. These alternative sands coat and perform significantly differently from silica sand of the same size and distribution. Moreover, a conundrum remains in the determination of the optimal shell cure temperature when the sand is opaque. What is an optimal cure color on the black sand disc-shaped specimen Fig. 3?

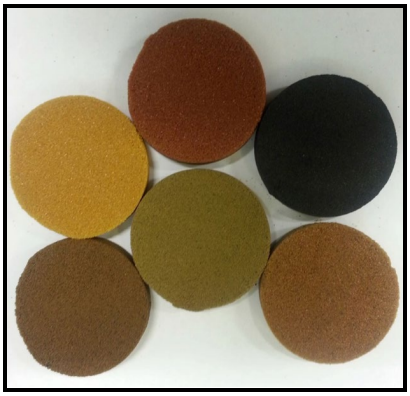

Figure 3. A complete cure is visually indicated by a degree of golden yellow to brown on a cure color chart.

SHELL ATTRIBUTES

One of the remarkable aspects of the shell process is its ability to successfully utilize almost any type of aggregate used in the foundry to make cores and molds. Shell formulations are made specific to the core, mold or casting requirements and the coated sand is partially cured/polymerized in the coating process, but it remains the only available resin coated sand that is dry and flowable. Variations can be sand type, resin type and percent used (1.0-5.5%), plasticizers, and additives specific to the end use as a solid/hollow core or thin mold. Additives can be custom blended into the sand formulation during the coating process whether it is clay, oxides, inhibitors, or additives for shakeout. The coating technology for shell sand has been well documented by Kerns et al.[6]

Shell has several advantages for the end user, in the cured state, shell cores are completely thermoset and are typically not prone to plastic deformation with the heat experienced during casting. Most shell cores are hollow and molds thin and lightweight. This can result in significant savings in sand usage, handling equipment and waste in addition to improved employee ergonomics and safety.[6] Moisture in the shell sand, either by condensation or introduced in the air line, will inhibit the sand's ability to flow and achieve full density, causing problems such as lower strength, peelback, or a delamination defect in shell sand. There are no concerns about bench life during a downtime, once the core or mold is made it has unlimited shelf life and is unaffected by moisture.[6]

SHELL AERATION TECHNOLOGY

The free-flowing characteristics of shell process sand in most cases can provide the required quality casting finish with coarser, more permeable sand that allows cores to be blown with lower blow pressures than might be required with an alternative wet process. This generally results in reduced wear on tooling surfaces.

The conventional shell sand filling methods are gravity or high blow. These methods are limited and, depending on application, can result in insufficient filling of shell sand to a complicated shape or deep pockets of small diameter. Such inconsistencies in shell cores and molds ultimately will lead to casting defects. An aeration shell sand filling system makes it possible for free-flowing resin coated shell sand to fill complex shapes, deep pockets, and thin sections within tooling that heretofore were not possible by conventional shell core making and molding methods such as gravity and high-pressure blow.[2] With the aeration sand filling method, the molding sand is fluidized, the flowability is greatly increased and the low-pressure aeration air encourages smooth sand feeding. Furthermore, since the open area of the blow nozzle is large, the speed of sand projection through the nozzle is much lower than with conventional high-pressure sand blowing methods. Consequently, in the aeration sand filling method, the sand with a low density falls on the pattern surface slowly and gently, as opposed to being blasted out at high speed.[2] Accordingly, the bridge-forming phenomenon at the area with complicated shape patterns and at the mouth of small size pockets is minimized. The sand streams down smoothly riding on the aeration air toward vents, and the bulk density is increased by the airflow effect. The composite actions of these effects make it possible to achieve high-density sand filling to the areas with complicated configurations and pockets having a small diameter.[2]

THERMAL DISTORTION TESTING (TDT)

The thermal distortion tester (TDT) uses disc-shaped specimens to compare chemically bonded sand systems (Fig. 4).[1-4] A sand composite is brought into direct symmetrical contact with a hot surface under pressure. The TDT uses a clean heating and control technology. The test temperature is variable and can be set to represent molten metal temperatures for the specific alloy for which the core/mold material will be used such as aluminum 760C (1400F), copper based alloys 1204C (2199F), cast iron 1450C (2642F), and steel 1600C (2912F).

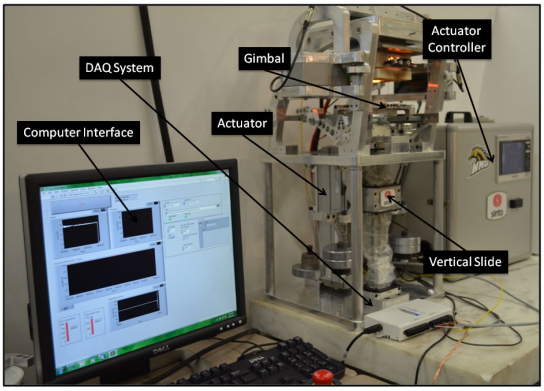

Figure 4. Thermal distortion testing (TDT) set up.

The TDT also has the capability to reproduce the pressures that sand binder systems will experience from molten metal filling and solidification in a mold. The duration of the test is set to mimic the time it takes for the metal skin to form at the mold wall interface. After thermal exposure, the test specimen is still intact allowing determination of additional valuable information that can be gained after thermal exposure, including strength, a visual analysis for cracks (which, in the metalcasting process, could result in penetration and/or veining), and a weight loss measurement that relates to pyrolysis of binder bridges and the amount of loose, unbonded sand generated at the mold metal interface as a result. The TDT was designed with the intent of obtaining deformation data for any sand binder system (natural or synthetic).

The TDT has the capability to represent the heat and pressures that sand binder systems will experience from molten metal filling and solidifying in a mold. The word "represent" must be emphasized since molten metal has never been used with the TDT, and there is no exact simulation of casting condition during the test.

Operating conditions of the TDT device are like those where a mass of molten metal is pressing against the mold wall in a pseudo-static state. The load (metallostatic head pressure) on the specimen is held constant, and the specimen can only move into or out of the face of the hot surface depending on whether the specimen is expanding or plastically deforming (Fig. 5). Holding the temperature of the hot surface constant during testing simulates the mass of molten metal.

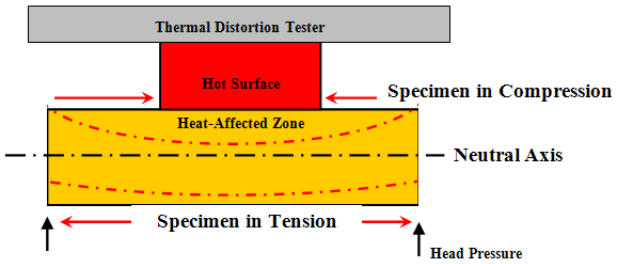

Figure 5. Thermal distortion test (TDT) stresses on the specimen.

All of the functionality of the device is accomplished through the use of several instruments, controllers, heating system, mechanical devices, and a computer that is used to record data. The TDT test procedure (AFS #3350-18-S) is documented in the "AFS Mold & Core Test Handbook"[4] and detailed descriptions of the instrument are provided in AFS Transaction.[1-4]

OBJECTIVE

The purpose of this project was to test and compare two resin coated shell sand systems (silica and ceramic) at an elevated temperature using the TDT. The thermal distortion curves will provide fresh data and results for foundry engineers and researchers regarding optimal cure parameters for shell resin coated sand systems.

METHODOLOGY

In the present work, a core box was aeration filled with free-flowing resin coated shell sand in order to produce disc-shaped specimens (50mm diameter x 8 mm thick). The specimens were used in a variety of physical, mechanical, and thermal tests. The testing procedure consisted of four major steps: 1) Preparation of the disc-shaped specimens and weight, 2) Scratch hardness, 3) Retained strength testing, and 4) TDT (observation of physical changes cracks and mass changes).

1. PREPARATION OF DISC SHAPED SPECIMENS

The properties of the shell resin coated sands used in this study are identified in Table 1. Apart from sand color, source, grand shape, and bulk density the properties after resin coating the sands are more or less the same. The shell resin coated sand was aeration filled into a cavity of an electronically heated core box (aluminum die tool) automatically (Fig. 6 (a)). Shell resin coated disc-shaped specimens were fabricated from either silica (S) or ceramic (C) sand. The disc-shaped specimens were cured within the disc-making tool maintained at three different cure temperatures just 14°C (25°F) apart (low 218C (424F), medium 232C (450F), and high 246C (475F). The low cure temperature was identified from the resin melt temperature (Table 1). For all specimens the curing process lasted 3 minutes after which the specimens were ejected from the tool (Fig. 6 (b)) and weighed on a digital balance.

Table 1. Properties of Resin Coated Shell Sands

Sand:	Round Grain Silica	Ceramic
Source	Oregon, IL	Houston, TX
% Resin BOS	2	2
pH	7.0	6.6
Acid Demand (pH-7)	0.8	0.5
USA Sieve No.	(% Retained)	(% Retained)
6	0.0	0.0
12	0.0	0.0
20	0.0	0.0
30	1.16	0.0
40	0.05	0.10
50	1.66	0.05
70	20.94	16.48
100	48.06	44.96
140	22.60	29.86
200	4.68	8.29
270	0.70	0.25
Pan	0.15	0.00
Screens	3	3
AFS-GFN	79	82
Fines (%)	5.5	8.5
Bulk Density (g/cm^3)	1.76	2.12
Surface Area (cm^2/g)	206	222
Melting Point (°F)	218	218
LOI (%)	2.01	2.05
3 min. Transverse (psi)	34	37
3 min. Hot Tensile (psi)	102	105
Roundness/ Sphericity (Krumbein)	0.8/0.8	0.9/0.9
Shape	Rounded	Round
Magnification: X100	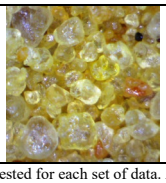	

Note: A total of 15 specimens were tested for each set of data. All specimens prepared and tested at Western Michigan University, Metal Casting Laboratory. Ambient conditions were temperature controlled at 20±1°C and relative humidity was controlled at 50%+/-2.

Aeration Sand Filling System

Aeration sand filling prevents segregation of free-flowing shell resin coated sands and allows a higher bulk density filling of the tool.[2] Ultimately, the process provides superior cured shell cores and molds compared to gravity filling and curing. Figure 6 shows the aeration shell sand filling and curing system built by Sintokogio, Ltd. This test machine is one eighth the size of an actual aeration shell molding machine. In this machine, a nozzle for delivering the resin coated sand from the aeration chamber is positioned on top of a core box (11 cm x 10 cm x 8 cm).

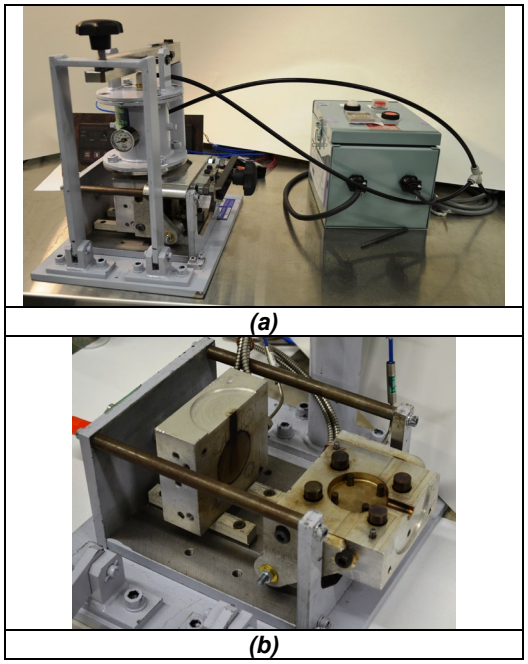

Figure 6. Shell aeration sand filling (a) and curing system (b).

Procedure

To operate the aeration sand filling system, dried compressed air was supplied via a regulated line and electrical power was switched on to power a microprocessor that controlled valves on a manifold. The manifold regulates time of aeration in the shell sand aeration chamber and time of pressurization air during filling. For shell sand filling, the aeration air is blown out from the aeration filter, which is attached to all surfaces of the aeration chamber. The aeration air fluidizes the shell sand. The friction resistance of shell sand against the filter surface is efficiently reduced and using low-pressure air to uniformly fill the core box. With this method, exhaust of the aeration air is routed through vents strategically machined into the parting line of the core box.[2]

The microprocessor controlled the timing and pressure for actuating the "pressure control" system that is set at an optimum level suited to a given core box. On the aeration shell sand filling system, aeration air 0.1 MPa for 1.0 second was used for all disc-shaped specimen. Heat curing, ejection and weighing of aeration specimens followed.

2. SCRATCH HARDNESS

Procedure

The scratch hardness tester is a direct reading instrument, and the test procedure (AFS 3318-00-S) is documented in the "AFS Mold & Core Test Handbook."[4]

3. RETAINED STRENGTH TESTING

Procedure

An impact testing machine (Tinius Olsen) equipped with a disc specimen holder (Fig. 7) was used to measure the strength of the sand specimens prior to and after the TDT. Impact strengths before TDT relate to handling of the core/mold material after core/mold production and prior to pouring. The impact strengths after TDT testing relate to shakeout/collapsibility characteristics.

The disc-shaped specimen was supported on its edge on a specimen holder on the impact testing machine. It was then subjected to impact energy by dropping a uniform load with a 2.00 mm thick rounded edge blade across its diameter. A load-cell electronically sensed the specimen failure, digitally displaying the results. The maximum energy to failure (joules) was recorded.

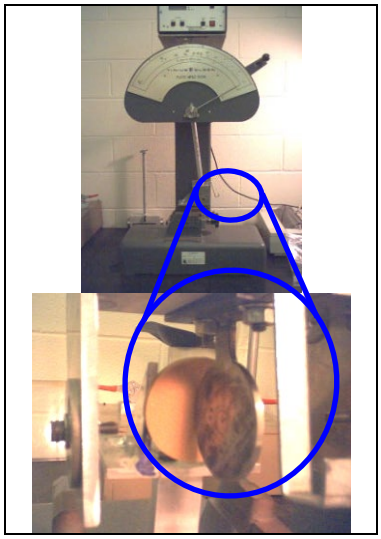

Figure 7. The impact tester and specimen holder.

4. TDT

Procedure

The test procedure (#AFS 3350-18-S) is documented in the "AFS Mold & Core Test Handbook."[1-4] Prior to elevated temperature exposure each specimen was weighed. Following elevated temperature exposure, the surface of the specimen was blown with 0.07 MPa (10 psi) air pressure to remove any loose sand grains. The specimens were re-weighed, and the percent change in

mass was recorded. Next, the specimens were automatically examined with a 3D Macroscope for discolorations, signs of thermally induced cracking and/or loss of sand where contact was made with the hot surface.[7]

Dimensional data regarding cracks and sand binder losses were collected using a one-shot, non-contact 3D Measuring Macroscope (3D-Macroscope) manufactured by Keyence (Model - VR 3100). This measurement system also allows the surface of the disc-shaped specimen to be captured (at ambient or elevated temperature).[7]

New measures have been incorporated into TDT. The authors have added a volatile organic compound (VOC) detection sensor to the test regime. A SGP30 hot-plate metal oxide sensor is used to measure the VOC concentration. Additionally, thermal sensors on the TDT have permitted the researchers to calculate a thermal gradient from the heat-affected-zone (HAZ) to the back side of a disc-shaped specimen post testing. Additionally, continuously monitoring the power to the hot surface along with parameters from the thermal gradient measurement allows a thermal conductivity to be calculated for a disc-shaped specimen.

RESULTS AND DISCUSSION

In this investigation, shell disc-shaped specimens were fabricated from either silica (S) or ceramic (C) sand. Specimens were cured at three cure temperatures just 14°C (25°F) apart; starting at the melt temperature of the resin. The high, medium, and low temperature cured specimens were tested and are designated as S_{Lo}, C_{Lo}, S_{Med}, C_{Med}, S_{Hi}, and C_{Hi}; respectively.

Mechanical and physical properties of the cured shell disc shaped specimens are shown in Table 2. The mass of C specimens is greater than the S sand specimens. However, the mass of S specimens showed less variability for all cure temperatures. Scratch hardness was always greater in the C sand specimens. However, the scratch hardness values were not significantly different for the various cure temperatures.

The specimens were impact tested (before and after TDT) to obtain baseline information for the toughness of the shell systems. In addition, all shell specimens were TDT at cast iron temperatures and the retained strength was measured (Table 2). Impact strength and retained strength was always greater in the C sand specimens and the toughness were not significantly different across the various cure temperatures. Still, shakeout of C specimens can/may prove to be a concern from castings. The retained strength in C specimens was similar in toughness to S specimens prior to elevated temperature exposure.

Table 2. Mechanical and Physical Properties of Shell Disc Specimens

Systems	Specimen Cure Temp. (± 1°C)	Specimen Mass (g)	Scratch Hardness (#)	Impact Strength (Joules)	Retained Strength (Joules)
S_{Lo}	218	23.76 (0.12)	75.50 (5.51)	1.03 (0.06)	0.73 (0.05)
C_{Lo}		29.00 (0.24)	88.33 (4.51)	1.19 (0.08)	1.07 (0.05)
S_{Med}	232	23.73 (0.12)	75.67 (1.15)	0.96 (0.01)	0.70 (0.06)
C_{Med}		28.98 (0.21)	87.50 (0.71)	1.16 (0.04)	1.02 (0.06)
S_{Hi}	246	23.69 (0.13)	71.67 (2.89)	1.00 (0.09)	0.68 (0.03)
C_{Hi}		28.96 (0.29)	92.00 (5.66)	1.19 (0.16)	1.00 (0.06)

Note: Values represent averages, and the standard deviations are shown in parentheses.

TDT

The TDT results are shown in Tables 3-5 and apart from distortion, change in mass, crack and fractures. Additional measures of thermal gradients, thermal conductivity, and VOC are provided. The TDCs for all systems (Figs. 8 and 9) tested showed undulations that indicate thermomechanical and thermochemical changes in the binder system at elevated temperature.[1-3]

For specimens tested at 1000C (1832F), the radial distortion (D_R) indicated an expansion trend especially for S compared C specimens (Figs. 8 and 9 (top)). It is important to point out that the rate of radial expansion was greater in S specimens over C by a factor of 10. Furthermore, cracks and fractures were detected only in S specimens; and beginning earlier in those specimens cured at higher temperatures.

For specimens tested at 1000C (1832F), the longitudinal TDC for S_{Lo} showed the most undulations (Fig. 8 (bottom)). For C specimens, the longitudinal distortion curves showed plastic deformation (downward movement of a TDC) (Fig. 9 (bottom)). The higher thermal gradient through the opaquer sand would encourage secondary polymerization and augment pyrolysis of the binder system; this was especially so for C_{Hi}.

TDT showed that regardless of sand type the higher shell sand cure temperatures from a resin melt temperature there was greater total thermal distortion (*TD*) (Tables 3 – 5). Furthermore, the C specimens reduced *TD* by ~50% when compared to S specimens.

Table 3. Thermomechanical Properties of Disc-shaped Specimens Cured at 218C (424F)

Shell Cured at 218 °C	Results of Thermal Dist. Testing @ 4.50 N for 90 seconds at 1000°C			Observation During Elevated Temp. Testing		Additional Thermal and Chemical Properties		
Resin Coated Sands	D_L Longitudinal (mm*sec)	D_R Radial (mm*sec)	T_D Total Dist. (mm*sec)	% Change in Mass	Cracks and Fractures	Thermal Gradient (°C/mm)	Thermal Conductivity (W/(m °C))	Total VOC (ppb)
S_{Lo}	-0.5470	5.8310	5.2840	0.253	Present after ~25 seconds	109 +/- 5	2.27 +/ 0.04	732.94
C_{Lo}	-2.3496	1.0476	3.3972	0.069	None	112 +/- 4	2.20 +/- 0.03	543.96

Note: Values represent an average of ten specimens.

Table 4. Thermomechanical Properties of Disc-shaped Specimens Cured at 232C (450F)

Shell Cured at 232 °C	Results of Thermal Dist. Testing @ 4.50 N for 90 seconds at 1000°C			Observation During Elevated Temp. Testing		Additional Thermal and Chemical Properties		
Resin Coated Sands	D_L Longitudinal (mm*sec)	D_R Radial (mm*sec)	T_D Total Dist. (mm*sec)	% Change in Mass	Cracks and Fractures	Thermal Gradient (°C/mm)	Thermal Conductivity (W/(m °C))	Total VOC (ppb)
S_{Med}	1.3252	6.8879	8.2131	0.213	Present after ~50 seconds	112 +/- 5	2.16 +/- 0.04	691.40
C_{Med}	-2.5420	0.5688	3.1108	0.070	None	113 +/- 4	2.18 +/- 0.02	551.25

Note: Values represent an average of ten specimens.

Table 5. Thermomechanical Properties of Disc-shaped Specimens Cured at 246C(475F)

Shell Cured at 246 °C	Results of Thermal Dist. Testing @ 4.50 N for 90 seconds at 1000°C			Observation During Elevated Temp. Testing		Additional Thermal and Chemical Properties		
Resin Coated Sands	D_L Longitudinal (mm*sec)	D_R Radial (mm*sec)	T_D Total Dist. (mm*sec)	% Change in Mass	Cracks and Fractures	Thermal Gradient (°C/mm)	Thermal Conductivity (W/(m °C))	Total VOC (ppb)
S_{Hi}	0.3452	9.1495	9.4947	0.125	Present after ~60 seconds	109 +/- 5	2.25 +/- 0.04	626.31
C_{Hi}	-3.1959	0.9585	4.1544	0.105	None	114 +/- 3	2.16 +/- 0.02	620.46

Note: Values represent an average of ten specimens.

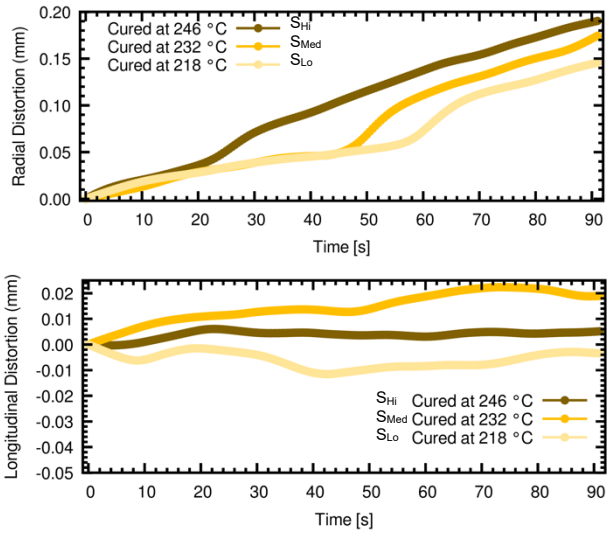

Figure 8. Radial (top) Longitudinal (bottom) TDC for S_{Lo}, S_{Med}, and S_{Hi}.

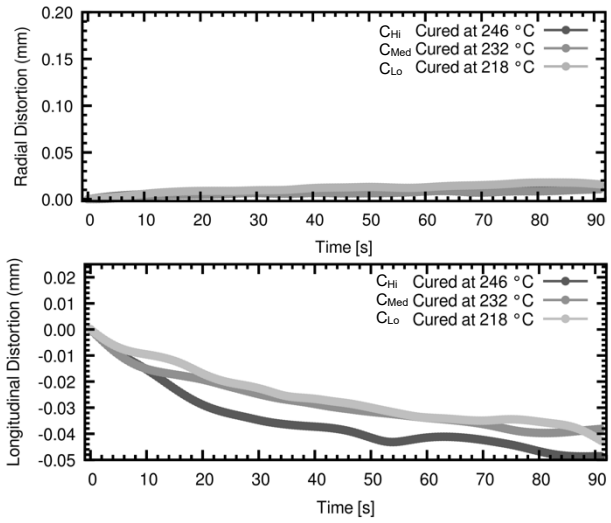

Figure 9. Radial (top) Longitudinal (bottom) TDC for C_{Lo}, C_{Med}, and C_{Hi}.

Mass Change

At the hot surface/specimen interface is where binder bridges pyrolyzed and sand grains broke loose.[1-3] The percent change in mass values (Tables 3-5) at the hot surface/specimen interface were minimal for shell resin coated sands; especially C specimens. Notably, expansion cracks were heard and macroscopically evident during TDT with only the silica specimens.

Table 6 shows images from a 3D Macroscope.[7] It is difficult to distinguish color differences among the as-cured images of either S or C specimens regardless of the cure temperature. After TDT and after any loose material was blown away, crack propagation was present in on the S specimens. The percent change in mass for all systems tested is shown in Tables 3-5.

Observations from the heat-affected-zone (HAZ) of specimens are shown in Table 6. The hot surface/specimen interface showed a black discoloration due to binder degradation. Losses at the HAZ may be indicative of the tendency to produce cuts and washes, erosion/inclusion type defects. There were minimal sand losses at the HAZ for all shell resin coated sand specimens tested. Interestingly, the losses for S specimens tested were lower at the higher cure temperatures; and the opposite for C specimens.

Table 6. Typical Shell Resin Coated Specimens Before and After TDT

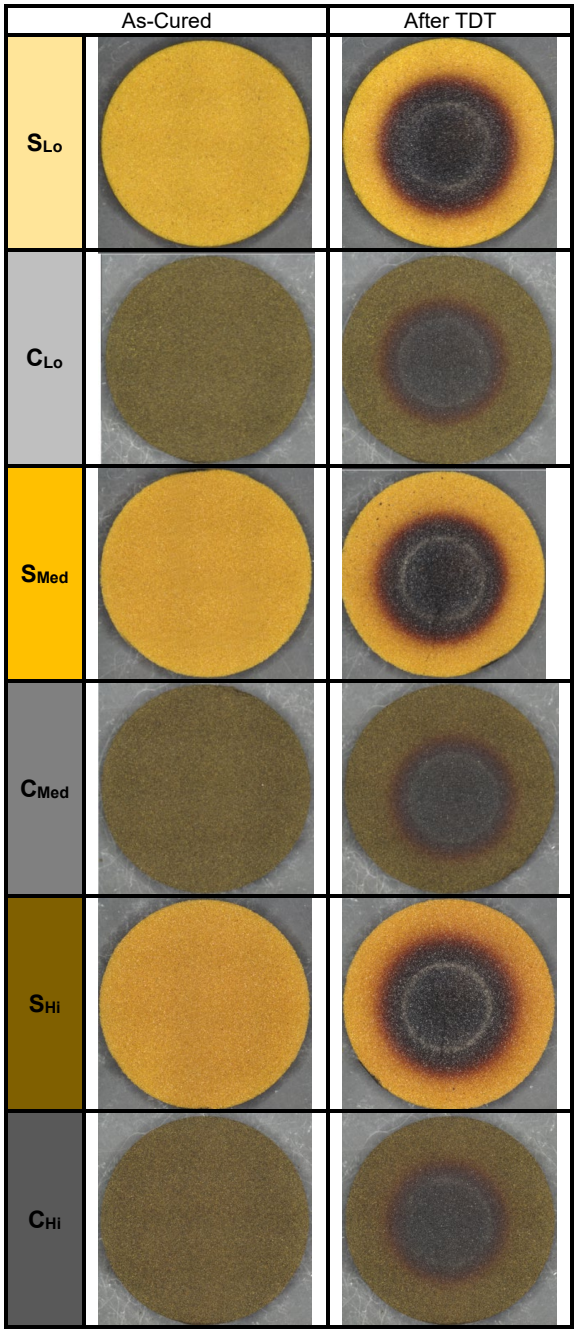

LIMITATIONS

The effects of cast iron chemistry on shell hot-box systems were not considered in this study. The work in this paper represents the data for two sand samples at ferrous superheat temperatures and pressure representative of a medium-size iron casting.

CONCLUSIONS AND RECOMMENDATIONS

The TDT provides thermomechanical data from shell resin coated disc-shaped specimens to identify the superior cure parameters. The pertinent data are in the forms of TDC, percent change in mass, and cracks on the surface of the test specimens. There were clear differences in distortion (longitudinal and radial) between the silica and ceramic shell resin coated sand specimens TDT at 1000C (1832F) with a 4.50 N (1.01 lb_f) load representing 20 cm (8 inch) cast iron metallostatic head pressure. With a shell aeration sand filling system, it is possible to produce cores and molds having superior mechanical properties (abrasion resistance, strength, and toughness), and thermal stability especially with the ceramic shell resin coated sand.

Further, work could be done at different loads and super-heat temperatures simulating various other cast alloys and pressures representative of larger or smaller castings. It is recommended that the new measures incorporated into TDT such as a thermal gradient, a thermal conductivity, and a volatile organic compound (VOC) detection from disc-shaped specimens be further investigated.

ACKNOWLEDGMENTS

Thanks to Carbo Ceramics, HA Group, Sintokogio, and WMU Metal Casting for support in this research.

REFERENCES

1. Ramrattan, S., Wells, L., Patel, P. et al., “Qualification of Chemically Bonded Sand Systems Using a Casting Trial for Quantifying Interfacial Defects,” Inter Metalcast 12, 214–223 (2018). https://doi.org/10.1007/s40962-017-0166-3
2. Ramrattan, S., J. Gray and A. Khoshgoftar, A., “Thermal and Mechanical Properties of Aeration Shell Sand,” *AFS Transactions*, 13-1452 (2013).
3. Ramrattan, S.N., Makin, R.A., Tay, Z. et al. , “Thermal Distortion Testing at Ferrous Superheat Temperatures,” Inter Metalcast (2024). https://doi.org/10.1007/s40962-024-01295-8
4. “AFS Mold & Core Test Handbook,” 5th Edition, American Foundry Society (2020). https://hub.afsinc.org/s/product-details?id=a2Z2L000000gLuYUAU (Link last accessed 03-03-2025.)
5. Knop P.A., A., Pilato, L. A., “Phenolic Resins; Chemistry, Applications, Performance,” Springer-Verlag (1985).
6. Kerns, K.J., Thiel, J., “Reinventing Shell Technology: Making Good “Scents” of an Ageless Process,” *AFS Transactions*, 09-064, pp. 313-321 (2009).
7. Keyence, One-shot 3D Measuring Macroscope, VR-3100, www.keyence.com (Link last accessed 03-03-2025.)